Molecular Therapy
Nucleic Acids
Original Article

Reduced expression of miR-30c-5p promotes hepatocellular carcinoma progression by targeting RAB32

Zheng He,[1] Meng Tian,[1] and Xuan Fu[1]

[1]Department of General Surgery, Shiyan People's Hospital of Bao'an District, No. 11 Jixiang Road, Bao'an District, Shenzhen, 518108 Guangdong, China

Hepatocellular carcinoma (HCC) remains among the most lethal of human cancers, despite recent advances in modern medicine. miR-30c-5p is frequently dysregulated in different diseases. However, the effects and the underlying mechanism of miR-30c-5p in HCC are still elusive. Here, we show that miR-30c-5p is downregulated in HCC and significantly associated with survival and tumor size in patients with HCC. We demonstrate that aberrant miR-30c-5p markedly affects HCC cell proliferation and migration. Further experiments show that RAB32 is an essential target of miR-30c-5p in HCC. These studies highlight an important role of miR-30c-5p in growth and invasion of HCC and indicate that the miR-30c-5p-RAB32 axis is an important underlying mechanism.

INTRODUCTION

Hepatocellular carcinoma (HCC) is a devastating and common disease with the third highest mortality rate globally.[1] Many patients are first diagnosed at an advanced tumor stage because of its malignancy.[2] Although significant progress in our understanding of HCC has been achieved in recent decades, there are no effective methods for patients with late-stage HCC or tumor recurrence after surgical resection.[3] The prognosis of patients remains poor. Therefore, there is an urgent need to identify novel biomarkers for early diagnosis and develop new therapeutic strategies for thoroughly understanding HCC cancer biology.

RAB32, a small GTPase, is a multifunctional vesicle-associated protein.[4] It is well established that RAB32 is involved in the biogenesis of endosomal organelles, such as forming autophagic vacuoles or lysosome-related organelles.[5,6] Although recent studies have reported that endosomal trafficking factors play a critical role in proliferation and invasion in multiple types of cancers, little is known about the physiological functions and regulated way of RAB32 in HCC.

MicroRNA (miRNA) is a type of short-chain non-coding regulatory RNA.[7] Thousands of miRNAs have been annotated in the human genome since the first report, which play a vital role in immune regulation, cell differentiation, and cancer progression.[8,9] Mature miRNAs are localized to the RNA-induced silencing complex (RISC), where they direct the complex to target 3′ untranslated region (UTR) of mRNAs, preventing mRNA translation or causing its degradation.[10,11] MiRNAs have complicated effects on cancer: some have been shown to promote tumor progression by directly acting on pro-apoptotic or anti-proliferative transcripts; meanwhile, some play a critical role in tumor-suppressing effects, which have been shown to inhibit the expression of genes that control cell differentiation or apoptosis.[12] Among the miRNAs, miR-30c-5p plays both oncogenic and tumor-suppressing roles in multiple cancer types. For example, it was reported that miR-30c-5p was significantly decreased in gastric cancer, which suppressed invasion and metastasis by targeting MTA1.[13] Exosome-derived miR-30c-5p relays anti-metastatic effects as a biomarker of clear cell renal cell carcinoma that inhibits progression by targeting HSPA5.[14] Although miR-30c-5p is considered a potential diagnostic indicator, it has also been reported to act as a tumor promoter in various tumor types.[15,16] Inhibiting miR-30c-5p expression offers a possible treatment of isolinderalactone-induced apoptosis for triple-negative breast cancer.[17] A previous study showed that the expression profile of serum miR-30c-5p was found to be deregulated in hepatitis C virus (HCV)-positive HCC.[18] However, the effects of miR-30c-5p in HCC are still elusive. Therefore, it is of great significance to reveal the precise molecular mechanism of miR-30c-5p for understanding the pathogenesis of HCC. The present study was designed to clarify the function of miR-30c-5p and its downstream targets in HCC.

RESULTS

The expression of miR-30c-5p is downregulated in HCC, and reduced miR-30c-5p expression is significantly associated with a poor prognosis

To assess the clinical significance of miR-30c-5p expression in HCC, we initially measured its expression in 32 paired HCC and adjacent tissue samples with clinicopathological features. Real-time PCR revealed that miR-30c-5p underwent downregulation in approximately 80% of cases (Figure 1A). The statistical results showed that miR-30c-5p was significantly downregulated in HCC compared with adjacent

Received 11 October 2020; accepted 31 August 2021;
https://doi.org/10.1016/j.omtn.2021.08.033.

Correspondence: Zheng He, Department of General Surgery, Shiyan People's Hospital of Bao'an District, No. 11 Jixiang Road, Bao'an District, Shenzhen, 518108, Guangdong, China.
E-mail: 805226494@qq.com

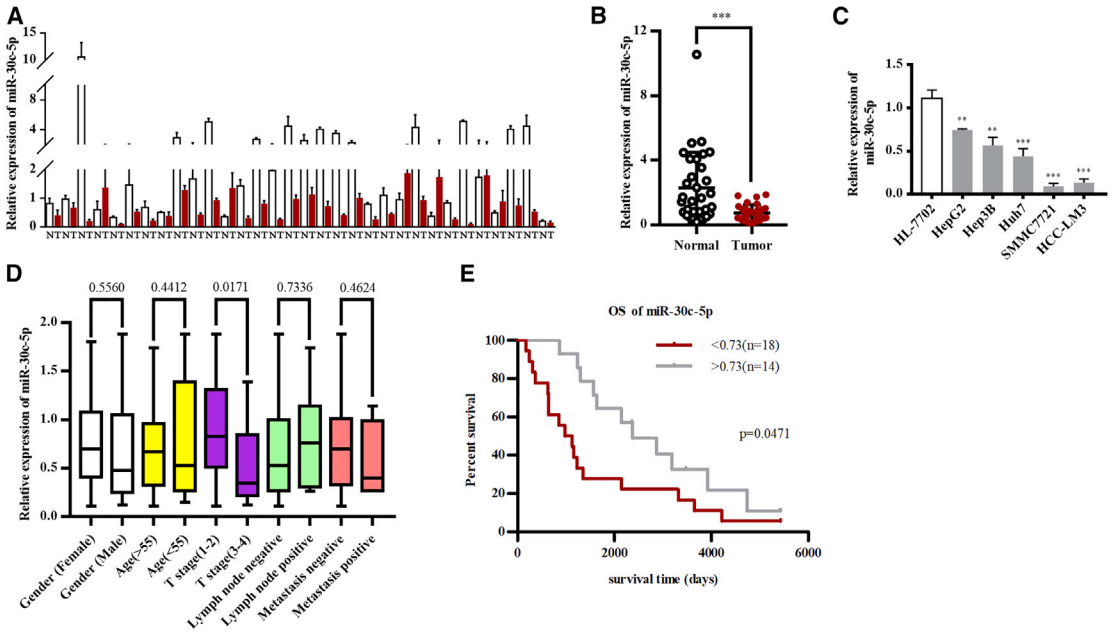

Figure 1. Expression of miR-30c-5p is downregulated in HCC, and reduced miR-30c-5p expression is significantly associated with a poor prognosis

(A) Real-time PCR analysis of miR-30c-5p in 32 paired HCC tissues. (B) Collected data from 32 paired HCC tissues show the expression of miR-30c-5p compared with that in normal tissue. (C) Real-time PCR analysis of miR-30c-5p in HCC cell lines as indicated. (D) Relative expression of miR-30c-5p in HCC with clinical and pathological stage are shown as boxplots. (E) Kaplan-Meier analysis of the correlation between miR-30c-5p expression and overall survival of HCC patients.

normal tissues (Figure 1B). Detection of miR-30c-5p expression was then performed in HCC cell lines and immortalized liver cell line. We found that miR-30c-5p expression was lower in every HCC cell line compared with normal liver cell line HL-7702 (Figure 1C). Clinicopathological analysis of miR-30c-5p expression revealed that reduced miR-30c-5p expression was significantly negatively associated with tumor size (T stage). However, no significant link was observed between miR-30c-5p level and age or sex (Figure 1D). Furthermore, Kaplan-Meier analysis showed that miR-30c-5p level was significantly associated with overall patient survival; those patients with lower miR-30c-5p levels had shorter overall survival (OS) (Figure 1E). Thus, these data indicate that the expression of miR-30c-5p is downregulated in HCC, and reduced miR-30c-5p expression predicts poor prognosis in HCC patients and may contribute to the progression of HCC.

miR-30c-5p inhibits cell growth in HCC cells

To determine the significance of miR-30c-5p in HCC, we performed loss-of-function and gain-of-function studies. According to the expression level of miR-30c-5p in HCC cell lines, we stably knocked down miR-30c-5p in high-miR-30c-5p-expressing HepG2 cells and overexpressed miR-30c-5p in low-miR-30c-5p-expressing SMMC-7721 cells by lentivirus (Figures S1A and S1B). We then examined the effect of miR-30c-5p on cell growth of HepG2 and SMMC-7721 cells. Cell viability and colony formation assays indicated that silencing miR-30c-5p expression significantly promoted cell growth of HepG2, and miR-30c-5p-upregulated SMMC-7721 cells showed largely impaired growth and formed fewer colonies compared with the control group (Figures 2A and 2B). To investigate the involvement of miR-30c-5p *in vivo*, we generated xenografts of subcutaneously implanted miR-30c-5p and control SMMC-7721 cells into nude mice. We found that miR-30c-5p overexpression in SMMC-7721 cells led to significant decreases in tumor size and weight (Figure 2C). From the third week, miR-30c-5p dramatically inhibited the growth rate of xenograft tumors (Figure 2D). Meanwhile, at week 5, mice in the miR-30c-5p-overexpressed group had slightly less body weight loss compared with the control group (Figure 2E). To further determine the growth of xenograft tumors, we carried out immunohistochemical (IHC) analysis for Ki67, which represents tumor proliferation. The results revealed that Ki67 was lower in the xenograft tumors of the miR-30c-5p-overexpressed group compared with the control group (Figure 2F). Collectively, these results demonstrate that miR-30c-5p inhibits HCC cell growth and tumorigenicity *in vitro* and *in vivo*.

miR-30c-5p reduces invasion of HCC cells

To evaluate the role of miR-30c-5p in the migration and invasion of HCC cells, transwell assays were first carried out. The results revealed that miR-30c-5p inhibition significantly enhanced the migration and invasion capacities of HepG2 cells (Figure 3A). In contrast, miR-30c-5p-overexpression cells showed significantly reduced ability to invade and migrate *in vitro* (Figure 3B). The wound-healing assays also showed that scratch-healing ability was enhanced considerably in miR-30c-5p-inhibited HepG2 cells, whereas overexpression of miR-30c-5p exerted the opposite effect on SMMC-7721 cells (Figures 3C and 3D). Also, we checked epithelial-mesenchymal transition

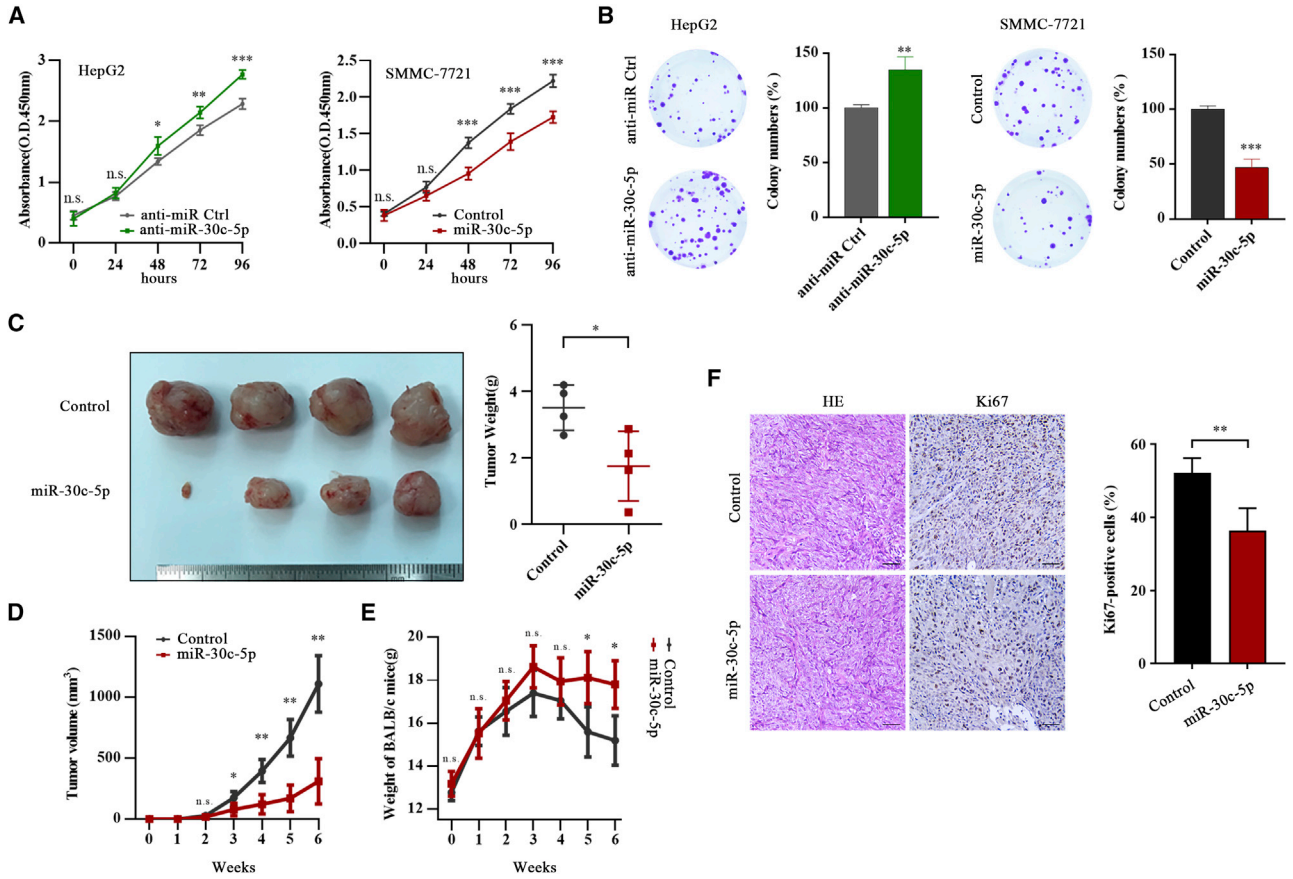

Figure 2. miR-30c-5p reduces invasion of HCC cells

(A) Viability of HepG2 cells stably expressing anti-miR-Ctrl, anti-miR-30c-5p, or SMMC-7721 cells stably expressing Control or miR-30c-5p detected using a CCK8 assay. (B) Representative images from the colony-forming assay (left panel) and colony number analysis (right panel) of HepG2 cells stably expressing anti-miR-Ctrl, anti-miR-30c-5p, or SMMC-7721 cells stably expressing Control or miR-30c-5p. All experiments were performed in triplicate, and data are presented as mean ± SD. (C) Images of subcutaneous tumors from the indicated groups (left panel) and weights of subcutaneous tumors from each group (right panel). (D and E) The tumor volume in each group and body weight of the mice were measured once a week from the time of tumor implantation. n.s., not significant. (F) IHC staining of H&E and Ki67 was performed.

(EMT)-related proteins, including E-cadherin, N-cadherin, β-catenin, snail, and vimentin, in our experiment. The result showed that anti-miR-30c-5p upregulated the expression of vimentin, β-catenin, snail, and N-cadherin and downregulated the expression of E-cadherin in HepG2 cells, indicating the activation of EMT. Meanwhile, miR-30c-5p inhibited the EMT process, as indicated by downregulation of vimentin, β-catenin, snail, and N-cadherin and upregulation of E-cadherin in SMMC-7721 cells (Figures 3E and 3F). These data indicated that miR-30c-5p plays an essential role in suppressing invasion and migration of HCC.

RAB32 is a key target gene of miR-30c-5p in HCC

To further ascertain the potential target underlying miR-30c-5p's regulatory role in cell growth and invasion, we performed RNA sequencing (RNA-seq) to analyze the global gene expression profile of HepG2 cells in miR-30c-5p-inhibited and control cells. Comparative gene expression profiles of miR-30c-5p-inhibited and control cells demonstrated that the expression of 989 genes was significantly changed, of which 56.5% (559 of 989) were observed to be upregulated (Figure 4A). We next used the computational prediction program TargetScan 7.2 to predict 1,576 potential target genes of miR-30c-5p.[19] Targets for the 14 genes were screened out with TargetScan 7.2, crossed with the 559 upregulated differentially expressed genes (Figure 4B). We then verified the results using real-time PCR and identified genes that were regulated by miR-30c-5p. Among these targets, RAB32 mRNA levels were upregulated in miR-30c-5p-inhibited cells and downregulated in miR-30c-5p-overexpressed cells (Figure 4C; Figure S2). Meanwhile, RAB32 protein levels were increased upon miR-30c-5p inhibition, and vice versa (Figure 4D). Also, the expression level of RAB32 was significantly downregulated in miR-30c-5p-overexpressed tumor xenografts (Figure 4E). Furthermore, we evaluated the 3′ UTR sequences of RAB32 and found that this complementary site is highly conserved in *Homo sapiens* (Figure 4F). This result implies that RAB32 may be directly epigenetically regulated by miR-30c-5p. Moreover, using a RAB32 3′ UTR reporter luciferase assay, we found that a significant increase of the relative luciferase activity was observed

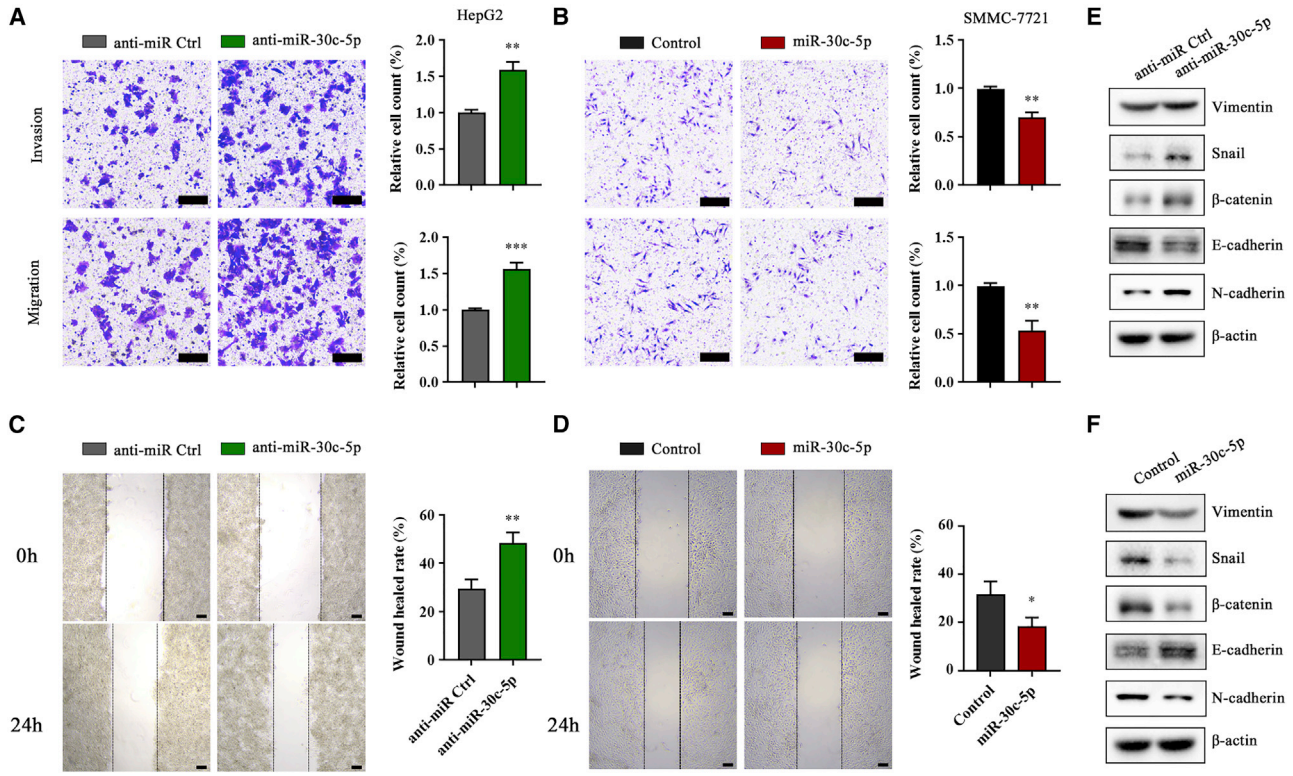

Figure 3. miR-30c-5p reduces invasion of HCC cells

(A) HepG2 cells stably expressing anti-miR-Ctrl or anti-miR-30c-5p were analyzed using a transwell assay with or without Matrigel. All experiments were performed in triplicate, and data are presented as mean ± SD. (B) SMMC-7721 cells stably expressing Control or miR-30c-5p were analyzed using a transwell assay with or without Matrigel. All experiments were performed in triplicate, and data are presented as mean ± SD. (C) HepG2 cells stably expressing anti-miR-Ctrl or anti-miR-30c-5p were analyzed using a wound-healing assay. All experiments were performed in triplicate, and data are presented as mean ± SD. (D) SMMC-7721 cells stably expressing Control or miR-30c-5p were analyzed using a wound-healing assay. All experiments were performed in triplicate, and data are presented as mean ± SD. (E and F) Expression of EMT-related proteins after inhibition or overexpression of miR-30c-5p in SMMC-7721 or HepG2 cells, respectively.

in miR-30c-5p-inhibited HepG2 cells. In contrast, upregulated miR-30c-5p largely reduced luciferase activity. Meanwhile, mutation of miR-30c-5p binding sites within RAB32 3′ UTR abolished the effects of miR-30c-5p or anti-miR-30c-5p (Figure 4G). Taken together, these data suggest that RAB32 is a direct target of miR-30c-5p in HCC cells.

RAB32 is responsible for the miR-30c-5p-related cell growth and invasion of HCC

Previous studies have concluded that miR-30c-5p is correlated with the cell growth and invasion capacities of HCC cells. To assess whether RAB32 is responsible for these capacities, we knocked down RAB32 in miR-30c-5p-silenced HCC cells (Figure 5A). RAB32 knockdown reduced cell viability and colony formation compared with control. Meanwhile, RAB32 silencing in the miR-30c-5p-inhibited cells abrogated the increase of cell viability and colony formation compared with that of the control cells (Figures 5B and 5C). Furthermore, the transwell and wound-healing assays revealed that RAB32 knockdown also significantly suppressed the miR-30c-5p inhibition-dependent increase of HCC cells' invasion and migration capacities (Figures 5D and 5E). To rule out the potential off-target effects of short hairpin RNA (shRNA), a shRNA-resistant RAB32 plasmid was construct and verified in RAB32-silenced HepG2 cells (Figure S4). These findings demonstrated that RAB32 is the effector and responsible for miR-30c-5p-related cell growth and invasion of HCC cells.

Aberrant expression of RAB32 in HCC

In order to verify the role of RAB32 in HCC, we next examined its expression in paired HCC and adjacent tissue samples. Real-time PCR in 16 cases with paired HCC and adjacent normal tissues revealed that the RAB32 mRNA level was significantly higher in HCC tissues compared with adjacent normal tissues (Figure 6A). Considering that miR-30c-5p regulates RAB32 at the RNA level, we hence analyzed a TCGA (The Cancer Genome Atlas) dataset including 423 HCC patients with RAB32 mRNA expression.[20] Given that RAB32 was the direct target of miR-30c-5p, we hypothesized that high RAB32 expression might be associated with poor survival. In fact, the RAB32 level in cancer was also higher on the basis of the TCGA/GTEx (Genotype-Tissue Expression) dataset (Figure S3).[21] Also, enhanced RAB32 level was significantly associated with advanced tumor stage (Figure 6B).

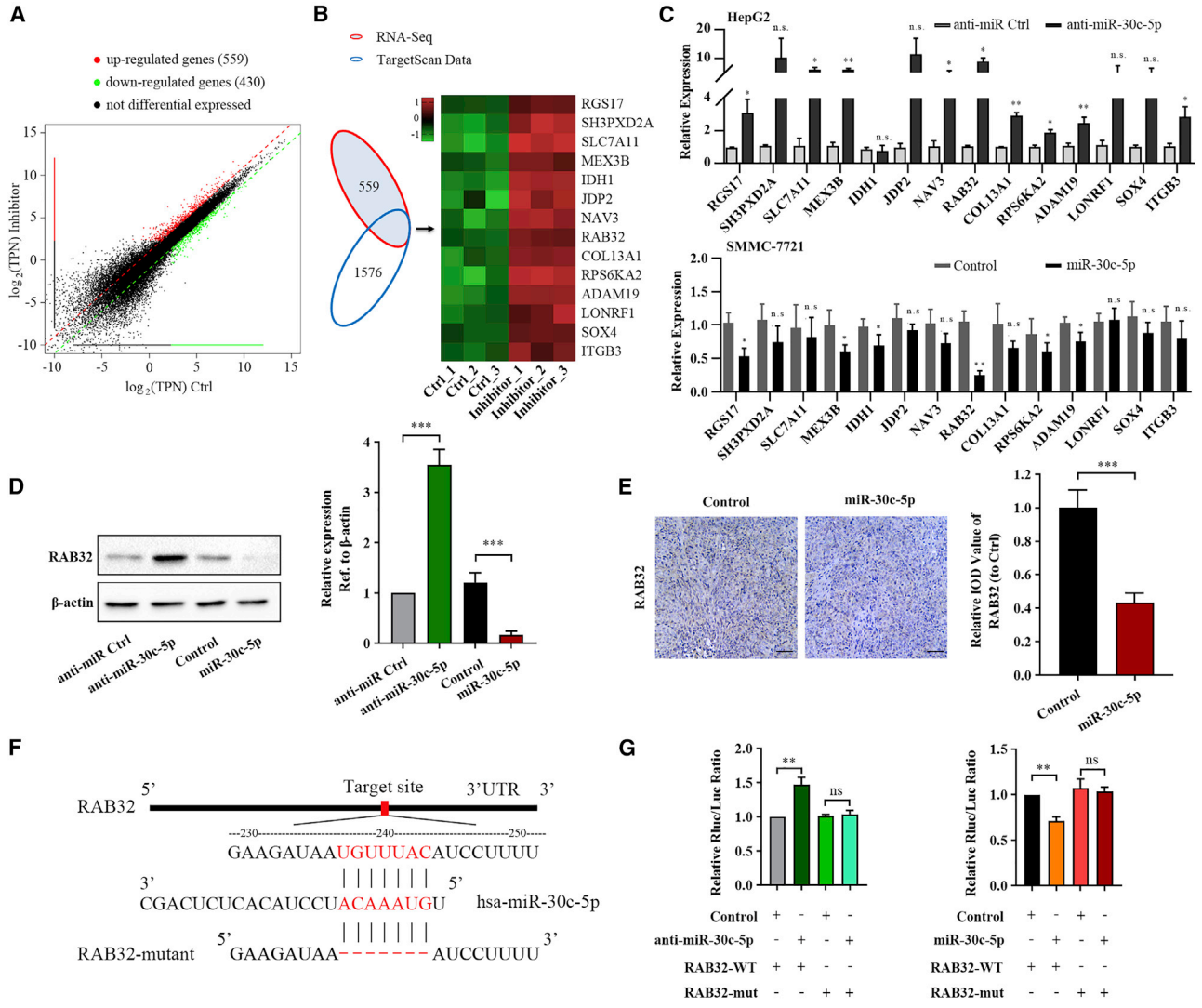

Figure 4. RAB32 is a key target gene of miR-30c-5p in HCC

(A) Differentially expressed genes with more than 2-fold expression change in HepG2 cells treated with anti-miR-30c-5p compared with anti-control. (B) Schematic diagram of miR-30c-5p downstream analysis.

(C) Real-time PCR analysis of the top 14 genes in HepG2 cells expressing anti-miR-Ctrl or anti-miR-30c-5p and in SMMC-7721 cells expressing Control or miR-30c-5p. (D) Western blotting of RAB32 in HepG2 cells expressing anti-miR-Ctrl, anti-miR-30c-5p, Control, or miR-30c-5p. (E) RAB32 expression level was quantified in control or miR-30c-5p over-expressed tumor xenografts. (F) Sequence alignment of miR-30c-5p with WT or mutant 3′ UTR of human RAB32 mRNA. Binding site and seed region of miR-30c-5p are indicated in red. (G) Effect of miR-30c-5p and anti-miR-30c-5p on the activity of WT or mutant RAB32 3′ UTR luciferase reporter plasmid measured using luciferase assay in HepG2 cells.

Moreover, Kaplan-Meier analysis showed that patients with higher expression of RAB32 had shorter OS, disease-free interval (DFI), disease-specific survival (DSS), and progression-free interval (PFI) than patients with lower RAB32 expression (Figures 6C–6F). Taken together, the expression of RAB32 is elevated in HCC, and the enhanced level of RAB32 predicts poor prognosis in HCC patients.

DISCUSSION

HCC continues to be a highly lethal malignancy, despite the use of surgical intervention and novel medication. HCC progresses insidiously and rapidly, so that some patients are already at an advanced tumor stage when first diagnosed. Hence the 5 year survival of HCC is still low.[1–3] As a non-coding RNA regulating gene expression at translational or posttranslational levels, miRNA is considered to play a key role in various diseases, especially in cancer.[22] Therefore, those miRNAs can be considered novel diagnostic and prognostic biomarkers.[23] In previous studies, the expression of miR-30c-5p was tissue specific, and it exerted both oncogenic and tumor-suppressing roles in different types of cancer.[13,14,16,17] It was reported that aberrant expression of miR-30c was a potential early diagnostic

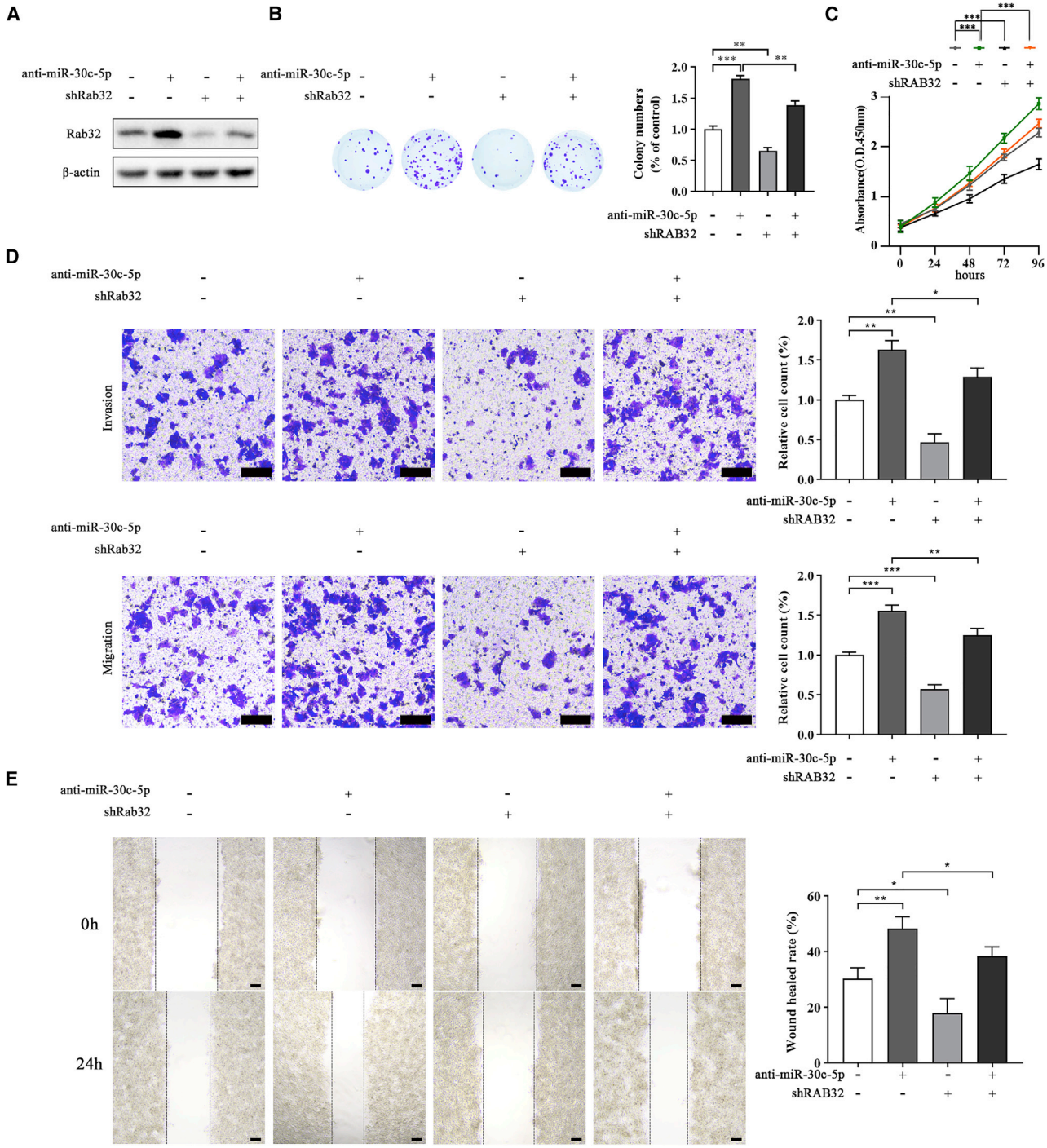

Figure 5. RAB32 is responsible for miR-30c-5p-related cell growth and invasion of HCC

(A) Relative expression level of RAB32 measured using western blot. (B) Representative images from the colony-forming assay (left panel) and colony number analysis (right panel) as indicated. All experiments were performed in triplicate, and data are presented as mean ± SD. (C) Viability of HepG2 cells with or without RAB32 knockdown in the absence or presence of miR-30c-5p inhibition analyzed using the CCK8 assay. (D) HepG2 cells with or without RAB32 knockdown in the absence or presence of miR-30c-5p inhibition were analyzed in a transwell assay with or without Matrigel. All experiments were performed in triplicate, and data are presented as mean ± SD. Scale bar: 200 μm. (E) HepG2 cells with or without RAB32 knockdown in the absence or presence of miR-30c-5p inhibition were analyzed in a wound-healing assay. All experiments were performed in triplicate, and data are presented as mean ± SD.

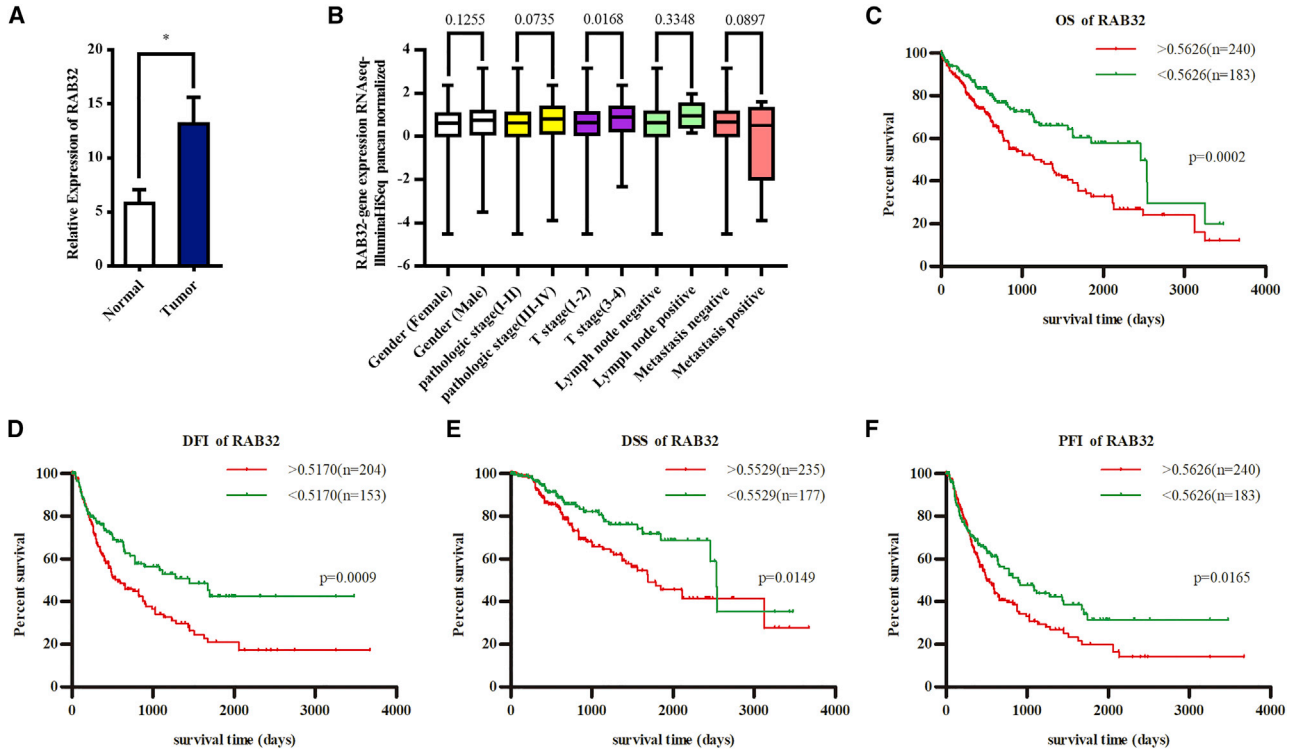

Figure 6. Aberrant expression of RAB32 in HCC

(A) Real-time PCR analysis of RAB32 in 16 paired HCC tissues. (B) Relative expression of RAB32 in HCC with clinical and pathological stage are shown as boxplots on the basis of TCGA data. (C–F) Kaplan-Meier analysis of the correlation between relative expression of RAB32 and overall survival, disease-free interval, disease-specific survival, and progression-free interval of HCC patients.

marker in HCC.[18,24] Meanwhile, miR-30c downregulation was associated with HCV core protein-induced EMT in HCC cells.[25] In our study, we demonstrated that the expression of miR-30c-5p is downregulated in HCC, and reduced miR-30c-5p expression predicts poor prognosis in HCC patients. This result is in line with our data that miR-30c-5p-overexpressed HCC cells showed reduced cell growth, invasion, and wound-healing capacities. Both sets of data thus indicate a tumor-suppressive function of miR-30c-5p in HCC.

MiRNA regulates target gene expression at translational or posttranslational levels via mRNA decay and translational repression, and each miRNA could potentially target multiple mRNAs.[26] Currently known targets of miR-30c-5p include MTA1,[13] HSPA5,[14] FOXO3,[27] SOCS3,[28] FASN,[29] Malic Enzyme 1,[30] SOCS1,[31] and PNS.[32] In order to explore the underlying mechanism, RNA-seq and the computational prediction program TargetScan were used for primary screening, and qPCR was used for verification in our study. RAB32, one of the 14 candidate targets screened out with TargetScan 7.2 crossed with the 559 upregulated differentially expressed genes, has been shown to be profoundly regulated by miR-30c-5p in HCC. We confirmed that forced expression of miR-30c-5p significantly reduced RAB32 expression at both the mRNA and protein levels in HCC cells. Furthermore, because of the typical seed sequence in the 3′ UTR of RAB32, RAB32 was a direct target of miR-30c-5p in HCC, as demonstrated by luciferase assays.

RAB32 is considered to regulate various intracellular membrane-trafficking events in many cell types.[4,5] Endosome-mediated membrane trafficking by RAB32 plays pivotal roles in protection events and mechanisms against several pathogenic microbial infections.[4,33] RAB32 was found to facilitate the assembly of HCV, and HCV infection concomitantly increased RAB32 expression at the transcriptional level.[34] RAB32 also plays a role in various type of cancers. Drizyte-Miller et al.[35] reported that RAB32 activated mTORC1 signaling, regulating autophagy and promoting cell proliferation, viability, and size in Hep3B and HeLa cells. Bao et al.[36] reported that RAB32 inhibited proliferation and migration and promoted apoptosis in K562 cells. In this study, we showed that RAB32 was involved in HCC progression, and it is the effector responsible for miR-30c-5p-related cell growth and invasion of HCC cells. Although it was reported that RAB32 inactivation due to hypermethylation was significantly associated with the oncogenic pathway of microsatellite-unstable gastrointestinal adenocarcinomas,[37] in our data we demonstrated that the expression of RAB32 is activated, and enhanced levels of RAB32 predict poor prognosis in HCC patients.

Accordingly, we propose that miR-30c-5p inhibits cell growth and invasion, and reduced expression of miR-30c-5p plays a crucial role in HCC progression by targeting RAB32 (Figure S5). Because of the

deficiency of effective therapy for treating HCC, the findings reported in this study suggest that miR-30c-5p and its target RAB32 may be promising targets in the future development of HCC treatments.

MATERIALS AND METHODS

Cell lines, samples, and chemicals

Human HCC cells (HepG2 and Huh7) were purchased from American Type Culture Collection (Manassas, VA). Human HCC cells (Hep3B, SMMC-7721, and HCC-LM3) and immortalized liver cell line (HL-7702) were kindly provided by the Department of Biliary-Pancreatic Surgery, Affiliated Tongji Hospital, Tongji Medical College, Huazhong University of Science and Technology. Cells were cultured in Dulbecco's modified Eagle's medium (DMEM) with 10% fetal bovine serum (FBS) at 37°C in a 5% CO_2 incubator. Thirty-two HCC samples and matched non-tumor tissues were consecutively collected from patients undergoing curative resection between September 2005 and May 2019 at the Department of General Surgery, The First College of Clinical Medical Science, China Three Gorges University, Yichang Central People's Hospital (Table S1). miR-30c-5p inhibitor, its control (referred to as anti-miR Ctrl), miR-30c-5p mimic, and corresponding negative control were purchased from RiboBio (Guangzhou, China). The primary antibodies used in this work were as follows: anti-E-cadherin (60335-1-Ig) was obtained from Proteintech Group (Chicago, IL); anti-RAB32 (ab251764) and anti-Ki67 (ab15580) were purchased from Abcam; and anti-β-actin (3700S), anti-N-cadherin (13116S), anti-Snail (3879P), anti-Vimentin (5741P), and anti-β-catenin (8480P) were obtained from Cell Signaling Technology (Beverly, MA).

Real-time PCR

Total RNA was extracted from cells or tissues using a TRIzol kit according to standard procedures. RNA was reverse-transcribed to cDNA using a TaqMan MicroRNA Reverse Transcription Kit (Applied Biosystems, Carlsbad, CA) or a PrimeScript Reverse Transcription Kit (Takara, Maebashi, Japan). Quantitative real-time PCR was performed using TaqMan MicroRNA Assays (Applied Biosystems) or the SYBR Green real-time PCR Premix (Takara) according to the manufacturer's instructions. All values were normalized to U6 or GAPDH endogenous controls, respectively, and run in triplicate. Primer of U6 and miR-30c-5p were chemically synthesized by RiboBio. The sequences of primers can be found in Table S2. Amplification and detection were performed using a CFX96 Real-Time PCR System (Bio-Rad, Hercules, CA).

Generation of stable cell lines

Lentiviruses harboring miR-30c-5p inhibitor, miR-30c-5p mimic, and their respective controls (referred to as anti-Ctrl and Control, respectively) were obtained from GeneChem (GenePharma, Shanghai, China). Transfection of lentivirus was performed according to the manufacturer's instructions. Briefly, after transfection with lentivirus for 48 h with 5 μg/mL polybrene (GenePharma), cells were cultured with 5 μg/mL puromycin (Sigma-Aldrich) for 2 weeks.

shRNA and transfection

To generate the shRNA plasmid, fragments of shRNA target were cloned into the pLKO.1. The specific RAB32 shRNA target was 5′-CCGGCATTTGAGGCAGTCTTAAAATCTCGAGATTTTAAGACTGCCTCAAATGTTTTTG-3′. Cells were transfected with Lipofectamine 3000 and Opti-MEM (Invitrogen, Carlsbad, CA) according to the manufacturer's instructions.

Cell viability and colony formation assays

For cell viability assay, cells were cultured in a 96-well plate with a concentration of 2,000 cells per well. At the indicated time points, the Cell Counting Kit-8 (Beyotime Institute of Biotechnology) was added to each well, and the cells were incubated at 37°C for 2 h, and then the plate was measured using a microplate reader (ELx800, BioTek, Winooski, VT) at 450 nm. For colony formation assay, cells (1,000/well) were seeded in a 6-well plate. After 14 days' culture, the cells were fixed in 4% paraformaldehyde, stained with 0.5% crystal violet, and photographed to quantify the colonies.

Transwell and wound healing assays

For transwell assay, 24-well transwell plates (8 μm pore size; Corning, Corning, NY) were used. Cells (1×10^5/mL) were suspended in 200 μL medium containing 0.1% bovine serum albumin into the upper chamber with or without Matrigel (BD Biosciences, San Jose, CA), and 500 μL of medium containing 10% FBS was added to the lower chambers. After 24 h co-culture, the cells on the top side of the chamber were scraped off, and the cells on the lower surface of the membrane were fixed in 4% paraformaldehyde and stained using 0.1% crystal violet. Then, the stained cells were counted under a Nikon light microscope (Nikon Corporation, Tokyo, Japan). Photographs of five random fields across three replicate wells under 200× magnification were captured for analysis. For wound-healing assay, monolayer cells were scratched with a sterile plastic tip with a 95% confluence rate, washed with PBS three times, and cultured for 24 h with serum-free medium. Photographs of five random fields across three replicate wells were captured for analysis under a Nikon light microscope.

RNA-seq

Total RNA from the indicated cell samples was sent to Sangon Biotech (Shanghai, China) for sequencing. Briefly, the RNA was sheared and reverse-transcribed using random primers to obtain cDNA, which was used for library construction. Sequencing was performed on the prepared library using the HiseqXTen platform (Illumina, San Diego, CA). After quality control of raw data, DESeq2 was used to analyze significantly differentially expressed genes with statistical cutoffs at $q < 0.05$ and $|\log \text{fold change (FC)}| > 2$. The 989 differentially expressed genes are listed in Table S3.

Protein isolation and western blot

Cells were washed with PBS twice and lysed in RIPA buffer (Boster Biological Technology, Wuhan, China) containing protease inhibitor

cocktail (Beyotime, Haimen, China) on ice for 30 min. After centrifugation at 20,000 × *g* for 15 min, supernatant was collected, and a bicinchoninic acid assay (BCA) kit (Beyotime) was used to quantify the protein. Fifteen micrograms of each sample was subjected to SDS-polyacrylamide gel electrophoresis (PAGE) and transferred to polyvinylidene fluoride (PVDF) membranes. After blocking with 5% skim milk for 1 h, membranes were incubated overnight at 4°C with primary antibodies (1:500–1:1,000). After washing with TBST three times, membranes were incubated with horseradish peroxidase secondary antibody (1:5,000; Beyotime) for 1 h and detected using SuperSignal West Pico Chemiluminescent Substrate (Thermo Fisher Scientific, Waltham, MA) and Image Lab software (Bio-Rad).

Luciferase reporter assay

To construct RAB32 3′ UTR wild-type or mutated luciferase reporter plasmids, the full-length 3′ UTR of RAB32 mRNA was cloned into psi-CHECK2 luciferase reporter vector (Promega, Madison, WI). The mutant Rab32 3′ UTR plasmid was constructed by deleting the miR-30c-5p-targeting sequence (UGUUUAC) in the 3′ UTR. Lipofectamine 3000 was used for co-transfection of reporter plasmids and miR-30c-5p, anti-miR-30c-5p, and control into HepG2 cells. After 48 h, luciferase activity was detected using the dual-luciferase reporter assay system (Promega) according to manufacturer's instructions.

Tumor xenografts

All experimental procedures were approved by the Institutional Animal Care and Use Committee of Shiyan People's Hospital of Bao'an Distict. Six-week-old BALB/c nude mice were randomly divided into two groups (n = 4 per group). Indicated stably transfected SMMC-7721 cells (2×10^6/mL) were subcutaneously injected into the upper right flank of nude mice. Tumor size and body weight of the mice were measured once a week from the time of implantation. Tumor volume was calculated using the following formula: volume (mm^3) = length × $width^2/2$. Six weeks after injection, all mice were sacrificed, and tumor xenografts were harvested and embedded in paraffin, cut into 5 μm sections, and subjected to immunohistochemistry staining for hematoxylin and eosin (H&E), Ki67, caspase-3, and Rab32.

Expression profiling in TCGA dataset

TCGA HCC mRNA gene expression data were downloaded from University of California, Santa Cruz (UCSC), Xena at https://xenabrowser.net/ and GEPIA 2 at http://gepia2.cancer-pku.cn. The gene expression profile was analyzed using the Illumina HiSeq pancan normalized pattern.

Statistical analysis

All data are presented as the mean ± SD. Significance was evaluated using Student's t test using GraphPad Prism 5 software (GraphPad, La Jolla, CA) and SPSS 22.0 software (SPSS, Chicago, IL). p values < 0.05 were considered to indicate statistical significance.

SUPPLEMENTAL INFORMATION

Supplemental information can be found online at https://doi.org/10.1016/j.omtn.2021.08.033.

AUTHOR CONTRIBUTIONS

Conception and Design, Z.H.; Acquisition, Analysis, and Interpretation of Data: Z.H., M.T., and X.F.; Writing, Review, and/or Revision of the Manuscript: Z.H.; Study Supervision, Z.H. All authors read and approved the final manuscript.

DECLARATION OF INTERESTS

The authors declare no competing interests.

REFERENCES

1. Torre, L.A., Bray, F., Siegel, R.L., Ferlay, J., Lortet-Tieulent, J., and Jemal, A. (2015). Global cancer statistics, 2012. CA Cancer J. Clin. *65*, 87–108.
2. Yang, J.D., Hainaut, P., Gores, G.J., Amadou, A., Plymoth, A., and Roberts, L.R. (2019). A global view of hepatocellular carcinoma: trends, risk, prevention and management. Nat. Rev. Gastroenterol. Hepatol. *16*, 589–604.
3. Llovet, J.M., Zucman-Rossi, J., Pikarsky, E., Sangro, B., Schwartz, M., Sherman, M., and Gores, G. (2016). Hepatocellular carcinoma. Nat. Rev. Dis. Primers *2*, 16018.
4. Ohbayashi, N., Fukuda, M., and Kanaho, Y. (2017). Rab32 subfamily small GTPases: pleiotropic Rabs in endosomal trafficking. J. Biochem. *162*, 65–71.
5. Hirota, Y., and Tanaka, Y. (2009). A small GTPase, human Rab32, is required for the formation of autophagic vacuoles under basal conditions. Cell. Mol. Life Sci. *66*, 2913–2932.
6. Hu, Z.Q., Rao, C.L., Tang, M.L., Zhang, Y., Lu, X.X., Chen, J.G., Mao, C., Deng, L., Li, Q., and Mao, X.H. (2019). Rab32 GTPase, as a direct target of miR-30b/c, controls the intracellular survival of Burkholderia pseudomallei by regulating phagosome maturation. PLoS Pathog. *15*, e1007879.
7. Eulalio, A., Huntzinger, E., and Izaurralde, E. (2008). Getting to the root of miRNA-mediated gene silencing. Cell *132*, 9–14.
8. Bartel, D.P. (2004). MicroRNAs: genomics, biogenesis, mechanism, and function. Cell *116*, 281–297.
9. Griffiths-Jones, S., Grocock, R.J., van Dongen, S., Bateman, A., and Enright, A.J. (2006). miRBase: microRNA sequences, targets and gene nomenclature. Nucleic Acids Res. *34*, D140–D144.
10. Chekulaeva, M., and Filipowicz, W. (2009). Mechanisms of miRNA-mediated post-transcriptional regulation in animal cells. Curr. Opin. Cell Biol. *21*, 452–460.
11. Hammond, S.M. (2015). An overview of microRNAs. Adv. Drug Deliv. Rev. *87*, 3–14.
12. Rupaimoole, R., and Slack, F.J. (2017). MicroRNA therapeutics: towards a new era for the management of cancer and other diseases. Nat. Rev. Drug Discov. *16*, 203–222.
13. Cao, J.M., Li, G.Z., Han, M., Xu, H.L., and Huang, K.M. (2017). MiR-30c-5p suppresses migration, invasion and epithelial to mesenchymal transition of gastric cancer via targeting MTA1. Biomed. Pharmacother. *93*, 554–560.
14. Song, S., Long, M., Yu, G., Cheng, Y., Yang, Q., Liu, J., Wang, Y., Sheng, J., Wang, L., Wang, Z., and Xu, B. (2019). Urinary exosome miR-30c-5p as a biomarker of clear cell renal cell carcinoma that inhibits progression by targeting HSPA5. J. Cell. Mol. Med. *23*, 6755–6765.
15. Chang, J.T., Wang, F., Chapin, W., and Huang, R.S. (2016). Identification of microRNAs as breast cancer prognosis markers through The Cancer Genome Atlas. PLoS ONE *11*, e0168284.
16. Onyshchenko, K.V., Voitsitskyi, T.V., Grygorenko, V.M., Saidakova, N.O., Pereta, L.V., Onyschuk, A.P., and Skrypkina, I.Y. (2020). Expression of micro-RNA hsa-miR-30c-5p and hsa-miR-138-1 in renal cell carcinoma. Exp. Oncol. *42*, 115–119.
17. Yen, M.C., Shih, Y.C., Hsu, Y.L., Lin, E.S., Lin, Y.S., Tsai, E.M., Ho, Y.W., Hou, M.F., and Kuo, P.L. (2016). Isolinderalactone enhances the inhibition of SOCS3 on STAT3 activity by decreasing miR-30c in breast cancer. Oncol. Rep. *35*, 1356–1364.

18. Oksuz, Z., Serin, M.S., Kaplan, E., Dogen, A., Tezcan, S., Aslan, G., Emekdas, G., Sezgin, O., Altintas, E., and Tiftik, E.N. (2015). Serum microRNAs; miR-30c-5p, miR-223-3p, miR-302c-3p and miR-17-5p could be used as novel non-invasive biomarkers for HCV-positive cirrhosis and hepatocellular carcinoma. Mol. Biol. Rep. *42*, 713–720.

19. TargetScan 7.2 (miR-30-5p predicted targets) dataset. TargetScan Human. http://www.targetscan.org/vert_72/.

20. TCGA Liver Cancer (LIHC) dataset. UCSC Xena. https://xenabrowser.net/.

21. TCGA/GTEx dataset available within GEPIA2. GEPIA2. http://gepia2.cancer-pku.cn/.

22. Huang, W. (2017). MicroRNAs: biomarkers, diagnostics, and therapeutics. Methods Mol. Biol. *1617*, 57–67.

23. Mishra, P.J., and Merlino, G. (2009). MicroRNA reexpression as differentiation therapy in cancer. J. Clin. Invest. *119*, 2119–2123.

24. Shen, J., Wang, Q., Gurvich, I., Remotti, H., and Santella, R.M. (2016). Evaluating normalization approaches for the better identification of aberrant microRNAs associated with hepatocellular carcinoma. Hepatoma Res. *2*, 305–315.

25. Liu, D., Wu, J., Liu, M., Yin, H., He, J., and Zhang, B. (2015). Downregulation of miRNA-30c and miR-203a is associated with hepatitis C virus core protein-induced epithelial-mesenchymal transition in normal hepatocytes and hepatocellular carcinoma cells. Biochem. Biophys. Res. Commun. *464*, 1215–1221.

26. Iwakawa, H.O., and Tomari, Y. (2015). The functions of microRNAs: mRNA decay and translational repression. Trends Cell Biol. *25*, 651–665.

27. Li, P., Zhong, X., Li, J., Liu, H., Ma, X., He, R., and Zhao, Y. (2018). MicroRNA-30c-5p inhibits NLRP3 inflammasome-mediated endothelial cell pyroptosis through FOXO3 down-regulation in atherosclerosis. Biochem. Biophys. Res. Commun. *503*, 2833–2840.

28. Zou, Y.F., Liao, W.T., Fu, Z.J., Zhao, Q., Chen, Y.X., and Zhang, W. (2017). MicroRNA-30c-5p ameliorates hypoxia-reoxygenation-induced tubular epithelial cell injury via HIF1α stabilization by targeting SOCS3. Oncotarget *8*, 92801–92814.

29. Fan, J., Li, H., Nie, X., Yin, Z., Zhao, Y., Chen, C., and Wen Wang, D. (2017). MiR-30c-5p ameliorates hepatic steatosis in leptin receptor-deficient (db/db) mice via down-regulating FASN. Oncotarget *8*, 13450–13463.

30. Zhu, W., Wang, H., Wei, J., Sartor, G.C., Bao, M.M., Pierce, C.T., Wahlestedt, C.R., Dykxhoorn, D.M., and Dong, C. (2018). Cocaine exposure increases blood pressure and aortic stiffness via the miR-30c-5p-malic enzyme 1-reactive oxygen species pathway. Hypertension *71*, 752–760.

31. Wang, C., Shan, L., Qu, S., Xue, M., Wang, K., Fu, F., Wang, L., Wang, Z., Feng, L., Xu, W., and Liu, P. (2020). The coronavirus PEDV evades type III interferon response through the miR-30c-5p/SOCS1 axis. Front. Microbiol. *11*, 1180.

32. Wang, L., Chen, X., Wang, Y., Zhao, L., Zhao, X., and Wang, Y. (2020). MiR-30c-5p mediates the effects of panax notoginseng saponins in myocardial ischemia reperfusion injury by inhibiting oxidative stress-induced cell damage. Biomed. Pharmacother. *125*, 109963.

33. Solano-Collado, V., Rofe, A., and Spanò, S. (2018). Rab32 restriction of intracellular bacterial pathogens. Small GTPases *9*, 216–223.

34. Pham, T.M., Tran, S.C., Lim, Y.S., and Hwang, S.B. (2017). Hepatitis C virus-induced Rab32 aggregation and its implications for virion assembly. J. Virol. *91*, e01662-16.

35. Drizyte-Miller, K., Chen, J., Cao, H., Schott, M.B., and McNiven, M.A. (2020). The small GTPase Rab32 resides on lysosomes to regulate mTORC1 signaling. J. Cell Sci. *133*, jcs236661.

36. Bao, J., Li, X., Li, Y., Huang, C., Meng, X., and Li, J. (2020). MicroRNA-141-5p acts as a tumor suppressor via targeting RAB32 in chronic myeloid leukemia. Front. Pharmacol. *10*, 1545.

37. Shibata, D., Mori, Y., Cai, K., Zhang, L., Yin, J., Elahi, A., Hamelin, R., Wong, Y.F., Lo, W.K., Chung, T.K., et al. (2006). RAB32 hypermethylation and microsatellite instability in gastric and endometrial adenocarcinomas. Int. J. Cancer *119*, 801–806.